

An Investigation into the Effects of Deposition Orientation of Material on the Mechanical Behaviours of the Cementitious Powder and Gypsum Powder in Inkjet 3D Printing

P. Shakor^a, S. Nejadi^a, and G. Paul^b

^aCenter for Built Infrastructure Research, School of Civil and Environmental Engineering, University of Technology Sydney, Australia

^bCentre for Autonomous Systems, School of Mechanical and Mechatronic Engineering, University of Technology Sydney, Australia

E-mail: pshtiwan.shakor@student.uts.edu.au, {shami.nejadi, gavin.paul}@uts.edu.au

Abstract –

Three-Dimensional Printing (3DP) is widely used and continues to be rapidly developed and adopted, in several industries, including construction industry. Inkjet 3DP is the approach which offers the most promising and immediate opportunities for integrating the benefits of additive manufacturing technic into the construction field. The ability to readily modify the orientation angle that the printed material is deposited is one of the most advantageous features in a 3DP scaffold compared with conventional methods. The orientation angle has a significant effect on the mechanical behaviours of the printed specimens. Therefore, this paper focuses on printing in different orientations somehow to compare various mechanical properties and to characterise a selection of common construction materials including gypsum (ZP 151) and cement mortar (CP). The optimum strength for the gypsum specimens in compression and flexural strength was observed in the (0° and 90°) and (0°) in the X-Z plane, respectively. According to the experimental results, the compression and flexural strength for ZP 151 are recorded at (11.59±1.18 and 11.78±1.19) MPa and 15.57±0.71 MPa, respectively. Conversely, the highest strength in compression and flexural strength are observed in the (90°) and (0°) degrees in the X-Z plane for the cement mortar, respectively. Moreover, it has been discovered that the compression and flexural strengths for CP are recorded as 19.44±0.11 MPa and 4.06±0.08 MPa, respectively. In addition, the dimensional effect for various w/c ratio has been monitored and examined.

Keywords –

Inkjet 3DP; cement mortar (CP); gypsum (ZP 151); mechanical strength; dimensional precision.

1 Introduction

Generally, the most common method in civil engineering is to cast in place or use precast procedures to construct structural members. These structural members are cast using different materials such as concrete, and masonry [10], [12] and [16]. Given the ever-increasing need for speed, quality and tailored design in the construction industry and due to the advances in rapid prototyping, the procedures for constructing structural members need to be rethought and upgraded [18].

Owing to the earlier studies, three main techniques for the 3DP powder-bed process have been recognized [14], i) selective binder (cement) activation, ii) binder jetting and iii) selective paste intrusion, respectively [22] [17]. These process could be monitored via the online vision sensor to control the slurry printing process [26]. The selective binder activation is the process that is used in this paper, which is usually known as powder-bed printing (binder/inkjet printing) [19] [23].

Inkjet printing is a layer-by-layer procedure to complete the entire scaffold using the powder-based materials and an activator such as water, Figure (1).

In inkjet 3DP, there are many limitations while printing the objects. For example, [28] discussed a few limitations in the 3DP such as binder selection, powder reactions, post-processing bed manipulations and de-powdering. One of the major limitations in 3DP is the orientation angle which has been discussed in earlier studies for the plastic and poly-jet materials [25].

In the following subsections, the mechanical strength of the recommended powder (ZP 151) and the modified powder (CP) have been monitored and compared. Moreover, the printed element has been examined within the different inclined rates for different angles. Nevertheless, the maximum compressive strength has been obtained for (CP) and (ZP 151). For the flexural strength, the highest results that have been observed for both (CP) and (ZP 151) are reported. Finally, the conclusions about the experimental study are presented and the future works are discussed.

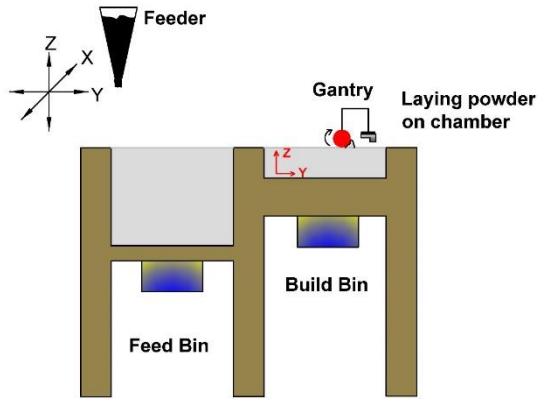


Figure 1. Schematic depiction of the powder-bed printing technique in inkjet 3D printing.

2 Materials and Specimens Preparation

2.1 Materials Composition

According to 3DSystems manual [2], the ZP151 contains (80-90%) of calcium sulphate hemihydrate ($\text{CaSO}_4 \cdot 1/2\text{H}_2\text{O}$). Moreover, Zb 63 is an aqueous solution and known as a binder, which has a high water content and humectant with the density of 1g/cm^3 [1].

In the previous study, [23] it has been found that the water/cement ratio (w/c) or (binder/powder) ratio can be determined by using Equation (1). The volume of a drop of binder will be measured according to the enveloped volume of powder in the build chamber of the printer.

$$Sat_{level} = \frac{V_b}{V_{EnvPowder}} \quad (1)$$

Where Sat_{level} is saturation level (w/c), V_b is the volume of the binder, and $V_{envpowder}$ the volume of the enveloped powder on the build chamber (build bin).

The alternative mix that has been used for printing contains as a percentage of total weight are 67.8% of Calcium Aluminate Cement (CAC) ranging sieve (75-150 μm), 32.2% of Ordinary Portland Cement (OPC) and 5% of fine sand. Figure (2) shows the histogram and curve of the density distribution of the custom-made and recommended materials versus particle size.

Figure (3) shows the modified mixing powder

(cement mortar CP), which replaces the ZP 151. It is noted that the mixing process has been completed using a Hobart mixer at a speed of 1450 RPM.

Moreover, the homogeneity and consistency of the powder materials are crucial factors that must be controlled when in pursuit of superior resolutions and results. Therefore, the speed of the mixer and the time of mixing are considered as a major contributor to the homogeneity of the powder and production of better quality 3DP objects.

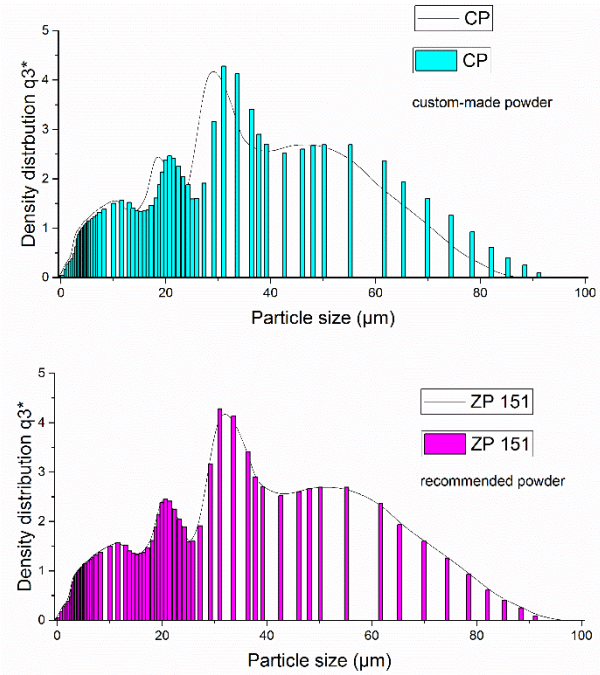


Figure 2. Histogram and curve of particle size distributions of ZP 151 and CP (custom-made) powder. *q3 is the unit standing for the density distribution of the total particles.

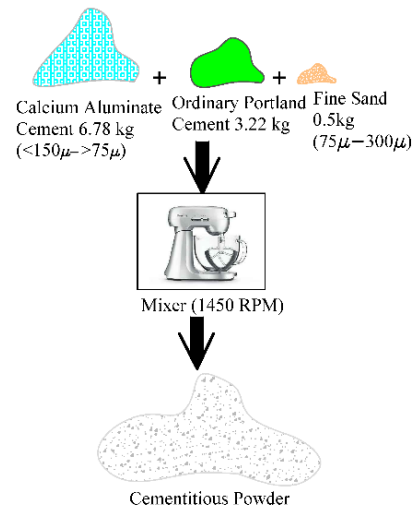


Figure 3. Schematic illustration of the process for preparing cementitious powder.

In addition, the optimum saturation level (w/c) of the binder for 3DP specimens has been reported [7]. According to the report, the highest saturation level is (S170C340) (Shell=170, Core=340), determined by Equation (1), which produces the highest result for the mechanical strength in 3DP specimens. The saturation level of the modified powder (S170C340) is equivalent to ($w/c=0.52$) in the manual mixing process for the cement mortar (CP) and ($w/c=0.46$) for the gypsum (ZP 151). The materials' chemical composition have been presented in Table (1).

Table 1. Chemical constituent percentages of the main materials in CP

Chemical Constituent % of Calcium Aluminate Cement			
Al ₂ O ₃	CaO	SiO ₂	Fe ₂ O ₃
≥ 37.0	≤ 39.8	≤ 6.0	≤ 18.5
Chemical Constituent % of Ordinary Portland Cement (General Purpose)			
Cement Clinker	CaCO ₃	CaSO ₄ .2H ₂ O	Clinker Kiln dust
>92%	0-7.5%	3-8%	0-2.5%

2.2 Specimen Preparation

The (ZP 151) has been directly placed into the 3DP (ProJet 360). However, the modified mix was prepared by a 20L Hobart mixer. The mixing procedure has been conducted in a dry mix state. Then, the prepared mix powder is placed into the inkjet 3D printer to print the mortar specimens. A Shimadzu load cell (AGS-X 50kN, Japan) testing machine was used to perform the mechanical tests at room temperature of ($22\pm 2^\circ\text{C}$) with a humidity level in the range of (60 ± 10) %.

Different orientation angles have been used to print the specimens ($0, 30, 37.5, 45, 90$)°. These angles have been selected because the halfway point of (0° and 90°), are the angle 45° . Commonly most of the shear rupture happens in concrete were between 0° and 45° [11]. Therefore, this paper focused on these angles between 0° to 45° . Figure (4) schematically shows the specimens with different orientation angles of print. Table (2) presents the name of the tests, numbers of samples, and CAD dimensions for both materials specimens

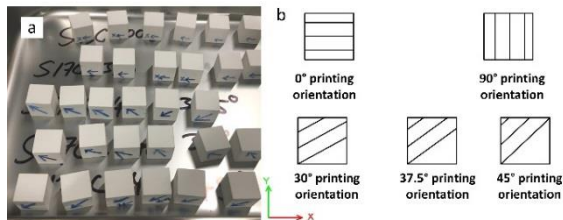


Figure 4. (a) Real-world images of the 3DP

cubes in ($0^\circ, 30^\circ, 37.7^\circ, 45^\circ, 90^\circ$) orientation (b) Drawing of 3DP cubes in ($0^\circ, 30^\circ, 37.7^\circ, 45^\circ, 90^\circ$).

3 Experimental Program

To determine the mechanical properties of the 3DP specimens, all the samples were designed in SolidWorks software as an STL file. Figure (5) shows the cubic samples in different orientation angles, which are printed at ($0^\circ, 30^\circ, 37.5^\circ, 45^\circ, 90^\circ$). It also shows the orientation angle of prepared specimens with regard to the X, Y, Z plane in the 3DSystems software. A mould ($20\times 20\times 20$), ($167\times 17\times 7$) mm used for casting the comparison, samples. All of the samples for compressive, and flexural strength tests have been prepared in a similar process.

The orientation angles in 3DP can be used in inkjet printing to create different geometries, optimize the mechanical strength of structure parts and optimize the number of layers to print an object.

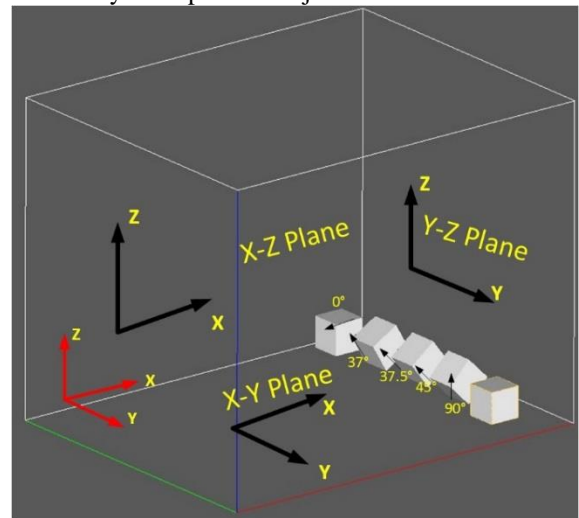


Figure 5. An illustration of the cube to be printed in different orientation angles according to X-Z plane.

Table (2) shows the type of tests, number of samples, and CAD drawing dimensions of the printing parameters.

Table 2. Tests with respect to the numbers and dimensions

Tests	No. of Samples	CAD Dimensions (mm)
Compression test	36	$20\times 20\times 20$
Three-point bending test	36	$167\times 17\times 7$
Dimensional accuracy	10	$20\times 20\times 20$

3.1 Testing and loading procedures

All the specimens have been tested using the universal testing machine (50 kN) with different rates of speed.

3.1.1 Effect of Dimensional Accuracy

The most vital features that distinguish the powder-based (inkjet) 3DP from the conventional casting method are the accuracy and dimensional precision of 3DP. Figure (6) shows the printed samples (cube and prism), which have been printed by inkjet 3DP: (a) left is mortar (CP) and (a) right is gypsum (ZP 151). Dimensions of the specimens have been measured by digital callipers with an accuracy of 0.01 mm and for the height, it has been used MeasumaX with an accuracy of ± 0.04 mm. Ten samples were used for the effects of dimensional accuracy test.

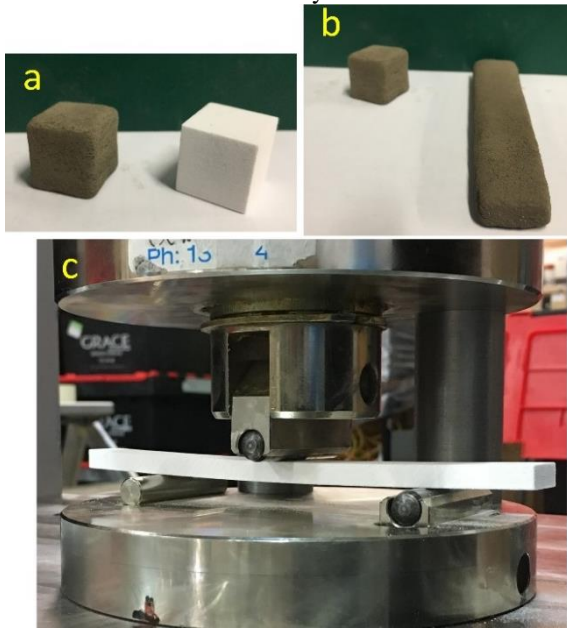


Figure 6. (a) 3DP cubic samples for CP and ZP 151, (b) 3DP cubic and prism CP sample, (c) 3DP prism gypsum while testing for three-point bending test.

3.1.2 Compressive Strength Test

One of the common factors that can be used to assess the durability of the concrete and mortar is its compressive strength [6]. Thus, the compression strength test has been performed for the 3DP samples according to the ASTM standard [6]. A total of 36 samples have been tested including 3 samples for each of orientation angles. The speed rate of the loading in the test was 0.833 kN/sec.

3.1.3 Flexural Strength Test

The specimens for the flexural strength test were prepared according to the ASTM standard [7]. A total of 36 samples have been printed using the manual mix,

including 3 samples prepared for each orientation angle. The speed rate of the loading in the test was 426 N/min.

3.1.4 Post-Processing Procedure

The curing and post-processing procedures are crucial to produce robust 3DP elements. After the element is printed, it should be kept for a minimum of 2 hours inside the build chamber of the printer so it can dry. According to the study of Feng et al. [8], specimens should be left for a further three hours to dry in an oven at 60°C after drying inside the build chamber. This leads to accelerating the solidifications and incremental stiffness of the gypsum scaffold (ZP 151). For that reason, the three hours curing in the oven has been implemented for ZP 151.

Curing of CP has been monitored using different trials and tests at the vitro. Accordingly, before and after curing in the water, CP has been drying at 60°C, results in higher compression strength in the CP specimens.

4 Results and Discussion

4.1.1 Effect of Dimensional Accuracy

The major advantage of the inkjet 3DP technique is a fabrication of structural components with complicated geometries without implementing costly formwork. The most vital aspect that distinguishes the inkjet (powder-based) 3DP from conventional casting method is the precision of printing. Figure (7) shows the results of the dimensional accuracy for the green cubic sample (green part) for the CP materials. Note that “green part” means a specimen that has been removed from the build chamber (build bin) prior to any post-processing.

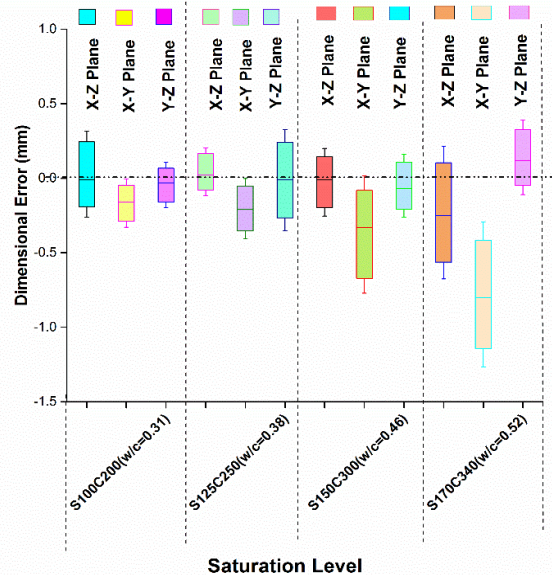


Figure 7. The relationship between dimensional accuracy and saturation level (w/c) for printed green cube CP specimens (CAD 20×20×20mm),

printed by ProJet CJP (304 nozzles). (Note: the box is the mean \pm standard deviation, and the whisker is \pm minimum and maximum).

The dimensional error can be found using Equation (2):

$$D_{error} = D_{printed} - D_{CAD} \quad (2)$$

Where D_{error} is a dimensional error, $D_{printed}$ is an actual printed dimension, and D_{CAD} is a CAD dimension.

Figure (7) also shows that in general the dimensional accuracy increases as the w/c is reduced for all planes. However, in the X-Y plane, a significant amount of undesirable deviation in the dimensional precision can be observed. These are lower than the nominal (CAD dimensions) that due to the inaccuracy of the printhead nozzle and closeness of the nozzles. This inaccuracy could lead overlapping and collision of the binder when it drops on the powder. Another reason is the chemical and physical characterization of the powder-to-binder and the ability of the powder for drop penetration. In addition, the printhead located on the fast axis rails which have a high rate movement. This can be counted as another important factor in the contribution of the accuracy of dimensions. The gantry holds all binder supply system, which is located on the fast axis rails in the printer.

4.1.2 Compressive Strength Test

In the previous study conducted by Shakor et al. [19], the porosity and voids in the cubic samples were investigated. The findings and optimum saturation level have been used in this paper to print and prepare all the scaffolds at the same saturation levels.

Figure (8) shows the porosity of the specimens versus the w/c ratio, where the highest saturation level (w/c) resulted in a reduction of the porosity percentage for both powders (CP) and (ZP 151). According to the study of Popovics et al. [15], the relationship between w/c ratio and porosity can be described by Equation (3);

$$p = 0.001a + \frac{w/c}{w/c+1/G} \quad (3)$$

Where p is the total porosity for the fresh cement, a is the air content by volume, G is specific gravity of cement and w/c is a water/cement ratio by mass. Consequently, an increase in w/c ratio means an increase in porosity of the sample, and resulted in a reduction in strength of the sample. However, this equation cannot be applied to the 3DP cementitious powder (CP) or gypsum (ZP 151). The printing of (CP) and (ZP 151) is completed in a layer-by-layer process. This technique is totally different from the manual mix process, which involves mixing the powder with water within one batch and vibrating it in the casting mould. The process of printing and post-processing applications has various effects on the mechanical properties and durability of the printed object. For example, the hygroscopic of the powder and electrostatic charge on the surface of the powder has a significant influence on the capability of powder to absorb moisture from the air.

This leads to an increase in the cohesion and a reduction in the flowability of the powder. Additionally, this property in the powder would affect the size of the specimen and change the mechanical properties of the specimen as well.

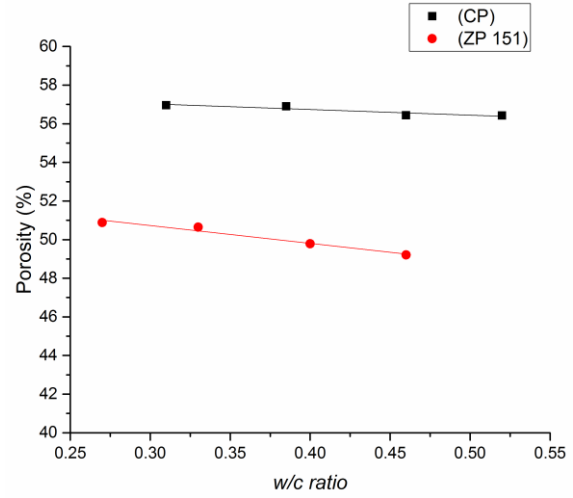


Figure (8) Relationship between porosity and w/c ratio for the mortar and gypsum printed scaffold.

Figure (9) illustrates the compressive strength of the specimen for the saturation level of S170C340. This saturation level is equal to a w/c of 0.52 in CP and 0.46 in ZP 151 using for all orientation angle. Accordingly, it shows the orientation angle of (90°) gives the highest value (19.44 ± 0.11 MPa) for CP after curing in an oven for 3 hours before and after wet curing, and a 7-day curing in water. This value is enough to build a structural member, which is cured only for 7-day. According to ACI code, a 7-day cure is counted as a 65% of the strength of mortar or concrete [3], while the compressive strength of mortar or concrete increases to about 99% strength in 28-day.

On the other hand, ZP 151 has recorded the highest result with an orientation angle of (0°) and (90°), i.e. when the printhead is parallel to the x -axis the highest result was recorded. This result matches with results reported by Asadi-Eydivand et al. [5]. However, this investigation needs further study to assess specimens in all three planes and axes. In addition, the rotating and changing scale of the specimens also needs further examination.

It is clear from the experimental results that the printing orientation angle has a major impact on the mechanical strength of the specimens, particularly in the cement mortar specimens. As shown in Figure (9) the printing orientation of (90°) has recorded the highest value of compressive strength which means the perpendicular directions has the optimum strength in the X-Z plane for cement mortar. However, the results for gypsum are slightly different since both angles (0° and 90°) could obtain maximum compressive strength. The results of the two angles are very similar to each other with

differences in the decimals range. Thus, it is highly recommended to print in the orientation angle of 90° for CP to achieve the highest compressive strength with concern to the flexural strength, which explaining in the following subsection.

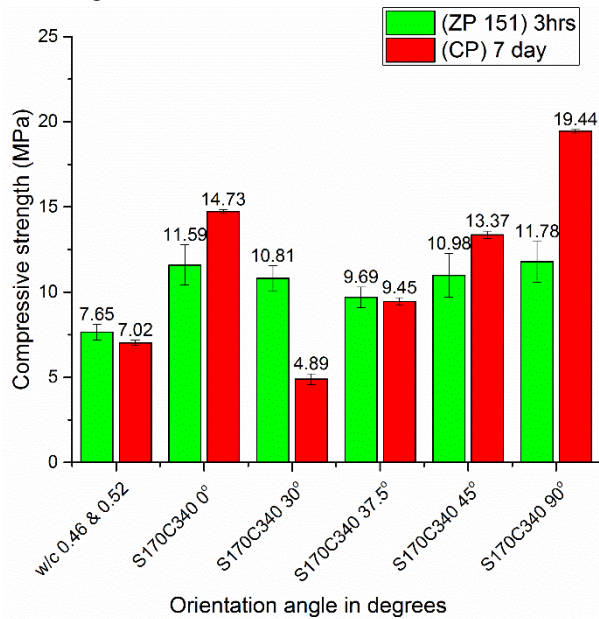


Figure (9) Compressive strength results for the ZP 151 cubes and CP cubes (average \pm standard deviation).

The halfway point between 0° and 45° is the angle 22.5° on the plane and is the most critical place for a crack in the concrete sample to begin. In this study, the angle 30° is the closest angle to 22.5° and is the reason for the emergence of a lower mechanical strength specifically in the cement mortar specimens. Further investigations are needed to check the results in different angles, e.g., 22.5° and 67.5°. The procedure used in this study is similar to a study conducted by [27], where tests were performed at a 22.5° angle for concrete blocks with dimensions (454×371)mm. However, the test results are quite different since the samples prepared in [27], were blocks joined by mortar, and not one continuous layer. Another reason is that the size, dimensions and properties of the materials are different which each have a significant impact on the outcomes of “orientational angle” results. Hence, the whole printed specimens are made from mortar and have a continuous longitudinal layer without the interruption of block joints. Therefore, the results would be different from conventional blocks.

4.1.3 Flexural Strength Test

Three-point bending tests have been conducted to evaluate the flexural strength of the printed gypsum and cement mortar specimens. Figure (10)

shows that in general, the flexural strength in gypsum is higher than the cement mortar specimens. According to the ACI code [4], the flexural strength of concrete is about 10% to 20% of the compressive strength result. Likewise, the result of CP in flexural strength after 7-day shows that the measured flexural strength is about 14% of compressive strength. Moreover, this could be due to the medium of the specimens, type, sizes, the volume of the particle size and duration of the curing.

Figure (10) shows flexural strength results quite opposite to the compressive strength result of both materials. As shown in Figure (9) the highest result is in CP specimens. However, in Figure (10) the results of the ZP 151 show higher values than the CP specimens. Previous studies have proved that using gypsum leads to an increase in bending and tensile strength [9]. The high percentage of lime content in fly ash with a high ratio of gypsum (1%), leads to a dramatic increase in the tensile strength [9]. Therefore, gypsum is acting as a flexible material and has great flexibility compared to the cement materials. In an earlier study by Lewry et al. [13], it has been proven that the reaction of water to plaster (gypsum), which is similar to the material ZP 151, with a 0.6 w/c ratio could gain about 12.2 MPa. This result is quite close to the manual mix of ZP 151 with w/c ratio of 0.46 in this study, which is 14.23 MPa. However, post-processing and purity of the materials have a significant effect on the result of the bending strength of gypsum materials.

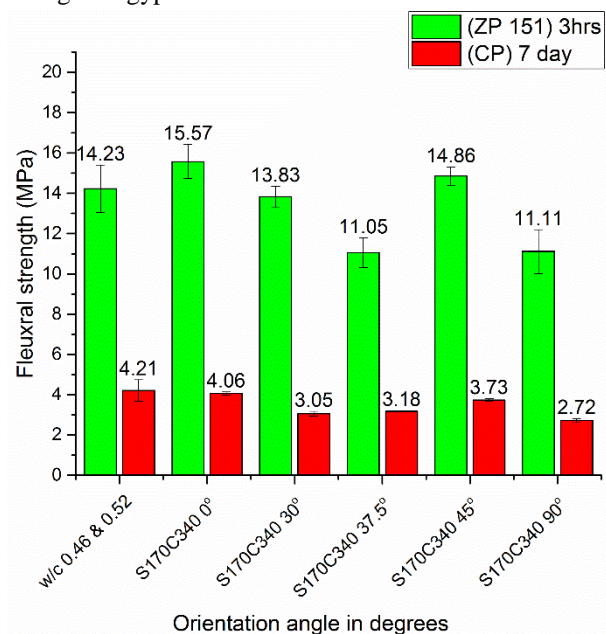


Figure (10) Flexural strength results for the ZP 151 cubes and CP cubes (average \pm standard deviation).

Furthermore, the result for the printed ZP 151 and CP samples are important due to the highest bending

strength recorded at the orientation angle of 0°. Meanwhile, the manual mix of CP in bending strength is slightly higher than the printed angle 0°. Therefore, the present study, the printing for the CP in the 0° and 90° are optimum angles to print for construction members because of the highest results achieved for compressive strength at angle 90° and highest results achieved for bending strength at angle 0°. This could be improved by adding reinforcement and later used for façade and cladding of the building [21] [24] [20].

5 Conclusion

3DP cubic and prism specimens have been printed with ZP 151 and CP materials. These specimens have been printed in different orientation angles to obtain better mechanical properties. In this paper, the dimensional accuracy for the CP printed specimens in the various w/c ratio (saturation levels) has been scrutinized and discussed. The results show that the x - y plane always has smaller dimensions than the other planes, this is due to the printhead direction, which is parallel to the x -axis and perpendicular to the y -axis. The printhead nozzles are too close and adjacent to each other and most probably the liquid binder overlapping and collide when dropping the droplet at high speeds. The other reasons could be due to the high capability of penetration of the water (binder) into the powder. Moreover, the dimensional accuracy is mostly decreased and highly variable while the w/c increases as a result of spreading high volumes of the water through the printhead. Particularly, spreading water in the y -axis is less than in the x -axis, which is perpendicular to the printhead, and vice-versa in the parallel direction (X -axis).

Furthermore, this study has investigated the effect of orientation angle on the printed structural members using CP (mortar) and ZP 151 (gypsum). The results show that this is an important factor that needs to be taken into consideration in the future studies of 3DP. The most appropriate orientations are 90° and 0° degrees for the strongest bending and compression strengths, respectively. In addition, this study is conducted to check the height of the printhead, number of the nozzles and spreading of the water (binder) while the printhead is moving on the powder bed and dripping water droplets at a fast speed. However, the effects of temperature and medium curing needs to be studied in detail for different powder types.

Acknowledgement

The authors would like to thank A/Prof. Anne Gardner and staff at the civil engineering laboratory for their support at the University of Technology Sydney. The authors would also like to gratitude to Kerneos Australia Pty Limited to provide CAC.

References

- [1] 3DSystems, ZB63 Safety Data Sheet, 2012.
- [2] 3DSystems, ZP151 Powder Safety Data Sheet, 2013.
- [3] ACI308R-01, Standard Guide to Curing Concrete, 2001.
- [4] A.c.i. ACI330R-01, Guide for Design and Construction of Concrete Parking Lots, 2001.
- [5] M. Asadi-Eydivand, M. Solati-Hashjin, A. Farzad, N.A. Abu Osman, Effect of technical parameters on porous structure and strength of 3D printed calcium sulfate prototypes, *Robotics and Computer-Integrated Manufacturing* 37 (2016) 57-67.
- [6] ASTM C39, 39, Standard test method for compressive strength of cylindrical concrete specimens, ASTM International (2001).
- [7] ASTM C293/C293M, 293 Standard Test Method for Flexural Strength of Concrete (Using Simple Beam With Center-Point Loading), ASTM Standard (2002).
- [8] P. Feng, X. Meng, J.-F. Chen, L. Ye, Mechanical properties of structures 3D printed with cementitious powders, *Construction and Building Materials* 93 (2015) 486-497.
- [9] A. Ghosh, C. Subbarao, Tensile strength bearing ratio and slake durability of class F fly ash stabilized with lime and gypsum, *Journal of Materials in Civil Engineering* 18 (1) (2006) 18-27.
- [10] H. Haroglu, Investigating the structural frame decision making process, © Hasan Haroglu, 2010.
- [11] N.M. Hawkins, Simplified shear design of structural concrete members, Transportation Research Board, 2005.
- [12] K.S. Kumar, P. Premalatha, K. Baskar, G.S. Pillai, P.S. Hameed, Assessment of Radioactivity in Concrete Made with e-Waste Plastic, *Journal of Testing and Evaluation* 46 (2) (2017) 1-6.
- [13] A.J. Lewry, J. Williamson, The setting of gypsum plaster, *Journal of Materials Science* 29 (23) (1994) 6085-6090.
- [14] D. Lowke, E. Dini, A. Perrot, D. Weger, C. Gehlen, B. Dillenburger, Particle-bed 3D printing in concrete construction – Possibilities and challenges, *Cement and Concrete Research* (2018).
- [15] S. Popovics, J. Ujhelyi, Contribution to the concrete strength versus water-cement ratio relationship, *Journal of Materials in Civil Engineering* 20 (7) (2008) 459-463.
- [16] M. Rashidi, R.S. Ashtiani, J. Si, R.P. Izzo, M. McDaniel, A Practical Approach for the Estimation of Strength and Resilient Properties of Cementitious Materials, *Transportation Research Record* (2018) 0361198118769900.
- [17] P. Shakor, S. Nejadi, 3D Printed Concrete Evaluations by Using Different Concrete Mix Designs, *Recent Trends in Engineering and*

- Technology, Bangkok, Thailand, 2017.
- [18] P. Shakor, S. Nejadi, G. Paul, S. Malek, Review of Emerging Additive Manufacturing Technologies in 3D Printing of Cementitious Materials in the Construction Industry, *Frontiers in Built Environment* 4 (85) (2019).
- [19] P. Shakor, S. Nejadi, G. Paul, J. Sanjayan, A Novel Methodology of Powder-based Cementitious Materials in 3D Inkjet Printing for Construction Applications Sixth International Conference on the Durability of Concrete Structures, Whittles Publishing, Leeds, UK, 2018.
- [20] P. Shakor, S. Nejadi, G. Paul, J. Sanjayan, A. Nazari, Mechanical Properties of Cement-Based Materials and Effect of Elevated Temperature on 3-D Printed Mortar Specimens in Inkjet 3-D Printing, *ACI Materials Journal* 116 (2) (2019).
- [21] P. Shakor, S. Pimplikar, U. Ghare, Techno-Commercial aspects of use of glass fibre in construction industry, *Advances and Trends in Engineering Materials and their Applications*, Advanced Engineering Solutions (Ottawa, Canada) Montreal, Canada, 2011.
- [22] P. Shakor, J. Renneberg, S. Nejadi, G. Paul, Optimisation of Different Concrete Mix Designs for 3D Printing by Utilizing Six Degrees of Freedom Industrial Robot, 34th International Symposium on Automation and Robotics in Construction, Automation in Construction, Taipei, Taiwan 2017.
- [23] P. Shakor, J. Sanjayan, A. Nazari, S. Nejadi, Modified 3D printed powder to cement-based material and mechanical properties of cement scaffold used in 3D printing, *Construction and Building Materials* 138 (2017) 398-409.
- [24] P.N. Shakor, S. Pimplikar, Glass fibre reinforced concrete use in construction, *Int. J. Technol. Eng. Syst* 2 (2) (2011).
- [25] M. Sugavaneswaran, G. Arumaikkannu, Modelling for randomly oriented multi material additive manufacturing component and its fabrication, *Materials & Design* (1980-2015) 54 (2014) 779-785.
- [26] S. Sutjipto, D. Tish, G. Paul, T. Vidal-Calleja, T. Schork, Towards Visual Feedback Loops for Robot-Controlled Additive Manufacturing, in: J. Willmann, P. Block, M. Hutter, K. Byrne, T. Schork (Eds.), *Robotic Fabrication in Architecture, Art and Design 2018*, Springer International Publishing, Cham, 2019, pp. 85-97.
- [27] J.A. Thamboo, M. Dhanasekar, Behaviour of thin layer mortared concrete masonry under combined shear and compression, *Australian Journal of Structural Engineering* 17 (1) (2016) 39-52.
- [28] B. Utela, D. Storti, R. Anderson, M. Ganter, A review of process development steps for new material systems in three dimensional printing (3DP), *Journal of Manufacturing Processes* 10 (2) (2008) 96-104.